Lab on a Chip

PAPER

Characterization of red blood cell deformability change during blood storage†

Cite this: *Lab Chip*, 2014, **14**, 577

Yi Zheng,[ab] Jun Chen,[a] Tony Cui,[f] Nadine Shehata,[d] Chen Wang*[de] and Yu Sun*[abc]

Received 9th October 2013,
Accepted 19th November 2013

DOI: 10.1039/c3lc51151k

www.rsc.org/loc

Stored red blood cells (RBCs) show progressive deformability changes during blood banking/storage. Their deformability changes over an 8 weeks' storage period were measured using a microfluidic device. Hydrodynamic focusing controls the orientation and position of individual RBCs within the microchannel. High-speed imaging (5000 frames s^{-1}) captures the dynamic deformation behavior of the cells, and together with automated image analysis, enables the characterization of over 1000 RBCs within 3 minutes. Multiple parameters including deformation index (DI), time constant (shape recovery rate), and RBC circularity were quantified. Compared to previous studies on stored RBC deformability, our results include a significantly higher number of cells (>1000 cells per sample *vs.* a few to tens of cells per sample) and, for the first time, reveal deformation changes of stored RBCs when traveling through human-capillary-like microchannels. Contrary to existing knowledge, our results demonstrate that the deformation index of RBCs under folding does not change significantly over blood storage. However, significant differences exist in time constants and circularity distribution widths, which can be used to quantify stored RBC quality or age.

Introduction

In transfusion medicine, red blood cells (RBCs) collected from blood donors are stored and preserved in a blood bank. Every year in the U.S. and Canada, over 14 million units of RBCs are administered to more than 5 million patients.[1] Present regulations in Canada and the U.S. specify 42 days as the shelf life for stored blood.[1,2] However, it has been suggested that during storage red blood cells undergo morphological, structural, and functional changes, which may induce clinical complications and adversely affect patient mortality.[3–6] For instance, transfusion of RBCs stored for more than two weeks was found associated with a significantly increased risk of postoperative complications as well as reduced short-term and long-term survival of cardiac surgery patients.[7]

The degradation of stored RBCs is known as the *storage lesion*.[4] Although the clinical consequences of storage lesions remain controversial,[3] intensive research has shown how parameters, which govern RBCs' metabolic ability and oxygen delivery capacity, such as 2,3-DPG, potassium, pH, HbO_2 saturation, RBC ATP, RBC NO, SNO-Hb, and haemolysis, change over the life span of stored RBCs.[1,8–10] In addition to these biochemical properties, the biconcave shape and high deformability of RBCs are also crucial for their physiological activities and functionalities.

The study on the deformability of stored RBCs dates back to the 1960s. La Celle and Weed investigated the progressive alteration of stored RBC deformability using a micropipette.[11,12] The hydraulic pressure required to aspirate the RBCs through the micropipette was used as a deformability indicator. Their results show that the RBCs that remained biconcave disc-shaped during storage have a deformability similar to that of fresh RBCs; however, those RBCs that became more spherical had decreased deformability. Optical tweezers were also applied to characterize the deformability of 0 days and 35 days stored RBCs by optically stretching the cells, wherein higher membrane elasticity and viscosity were observed in 35 day old RBCs.[13] More recently, ektacytometry was used to study the deformability of stored RBCs. Ektacytometry consists of two rotating plates with a small gap in-between. RBCs adhere to the bottom of the gap,

[a] *Department of Mechanical and Industrial Engineering, University of Toronto, Toronto, ON, Canada. E-mail: sun@mie.utoronto.ca; Fax: +1 416 978 7753; Tel: +1 416 946 0549*
[b] *Institute of Biomaterials and Biomedical Engineering, University of Toronto, Toronto, ON, Canada*
[c] *Department of Electrical and Computer Engineering, University of Toronto, Toronto, ON, Canada*
[d] *Department of Pathology and Laboratory Medicine, Mount Sinai Hospital, Toronto, ON, Canada. E-mail: cwang@mtsinai.on.ca; Tel: +1 416 586 4469*
[e] *Department of Laboratory Medicine and Pathobiology, University of Toronto, Toronto, ON, Canada*
[f] *Department of Chemical Engineering and Materials Science, University of Minnesota, Minneapolis, MN, USA*
† Electronic supplementary information (ESI) available. See DOI: 10.1039/c3lc51151k

and shear stress elongates the RBCs. The extent of cell elongation is measured as an indicator of RBC deformability. Using ektacytometry measurements, the progressive elongation change of stored RBCs over 42 days storage period was reported, demonstrating that RBCs become harder to elongate when stored longer.[1,14–16]

Measuring the deformability of stored RBCs using micropipette and optical tweezers is tedious and skill-dependent. More importantly, the low measurement speed (minutes to tens of minutes for testing one cell) makes these techniques infeasible to obtain sufficient information of the highly heterogeneous blood cell population.[17–19] As stored RBCs age, the cells change their morphology progressively from biconcave to more spherical (spheroechinocytes).[5,10,20] Even for the cells within the same stored blood sample, their morphology change varies significantly. Hence, testing only a few cells from a blood sample cannot objectively reveal deformability changes of the sample.

Compared to micropipette and optical tweezers, ektacytometers are relatively easy-to-use. However, ektacytometry measurement is limited to approximately 50–60 RBCs per test. In ektacytometry, elongation index measured *via* laser diffraction is the only parameter for indicating RBC deformability.[21,22] The definition of elongation index becomes improper when RBCs' shapes become less regular.[23–25] Furthermore, ektacytometry requires RBCs to settle and adhere to the bottom of the ektacytometer chamber in order to elongate the cells under shear stress. This deformation mode is not physiologically relevant since *in vivo* RBCs are *folded* when flowing through human microcapillaries with diameters comparable to or smaller than RBCs.[26–28] It is known that the mechanical properties of RBCs can differ significantly when deformed under different modes (*e.g.*, extension or folding).[29,30]

This paper describes the *folding* of stored RBCs on a microfluidic device. Fresh and stored RBCs were pressure-driven to flow through microfluidic channels (cross-sectional area: 8 μm × 8 μm). Hydrodynamic focusing within the microchannel controls the orientation and position of individual RBCs. High-speed imaging (5000 frames s^{-1}) captures the dynamic deformation behavior of the cells, and together with automated image analysis enables the characterization of over 1000 RBCs within 3 minutes. Multiple parameters including deformation index (DI), time constant (recovery rate after an RBC exits the channel), and circularity of the individual cells were quantified. Compared to existing stored RBC deformability studies, our results include a significantly higher number of cells (>1000 cells per sample *vs.* a few to tens of cells per sample) and, for the first time, reveal deformation changes of stored RBCs when traveling through human-capillary-like microchannels. The correlation between deformability and morphology of stored RBCs is also reported.

System overview

Fig. 1(a) shows a schematic of the microfluidic device for studying RBC deformability changes during storage. The central channel is 160 μm long and has a cross-sectional area of 8 μm × 8 μm. The recovery region has a cross-sectional area of 200 μm × 8 μm, where the deformed RBCs gradually recover to their original shape. The channel length of 160 μm was chosen for ensuring the deformation of the RBCs has reached a steady state before exiting the channel to eliminate the influence of cell position variations on DI measurement, due to the frame rate limit (5000 fps). Two focusing channels are integrated to center and orient the RBCs. The loading and focusing channels are connected to a custom-developed precise pressure source using water tanks. When RBCs flow through the central channel, RBC images are captured by a high-speed camera (5000 frames s^{-1}) through an inverted microscope. Fig. 1(b) shows the dynamic process of RBC deformation. When the cell entered the channel, its position was close to one of the microchannel walls. After the focusing unit, the cell was centered and adjusted to the 'standing' orientation. It then underwent symmetrical shear stress, resulting in a parachute-like shape near the exit. When the cell exited the microchannel, shear stress was released, and the RBC gradually recovered to its original shape.

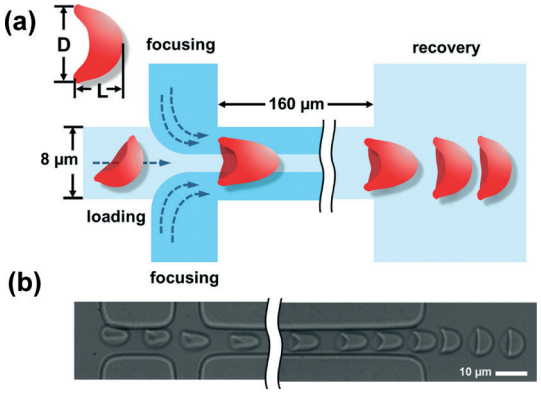

Fig. 1 (a) Schematic of the microfluidic device for studying deformability changes of stored RBCs. Hydrodynamic focusing centers the cell and adjusts it to the 'standing' orientation. The RBC is 'folded' into a parachute-like shape when pressure-driven through the 8 μm × 8 μm central channel. Deformation index (DI = *L*/*D*) is defined to measure RBC deformation (top-left). Time constant (tc) of each individual cell is determined by fitting DI value changes during the cell shape recovery process to an exponential function, after the cell exits the microchannel. (b) Experimental images showing the centering, orienting, folding, and shape recovering of an RBC.

In order to quantify the deformation behavior of RBCs, deformation index (DI) is defined as DI = *L*/*D* [see Fig. 1(a)] in the last frame of image right before the cell exits the microchannel and enters the recovery region (*i.e.*, last frame of image in the 8 μm × 8 μm channel). Recovery time constant (tc) is determined by exponentially fitting DI values with respect to time. Circularity, defined as circularity = 4π × area/perimeter^2 (circularity = 1 means a perfect circle), is measured experimentally in the last frame of image right before the cell exits the region of interest (as shown in ESI† videos) to depict the morphology of each stored RBC.

Methods and materials

Blood samples

Stored blood samples were collected using techniques consistent with the Technical Manual of the AABB (American Association of Blood Banks)[31] and used in experiments in accordance with a research protocol approved by the Mount Sinai Hospital Review Board. Briefly, venous blood samples (500 ml ± 10%) were collected from healthy donors in CP2D anticoagulant. After separation of plasma and buffy coat, the RBCs were suspended in saline-adenine-glucose mannitol (SAGM) (110 ml), and then stored in a blood bank refrigerator at 4 °C. For each test, an RBC aliquot was removed and tested at desired time intervals.[1,10] After an RBC sample was drawn from the aliquot, it was diluted with PBS with 1% w/v BSA (RBC sample : PBS = 1 : 100) and incubated for 10 min at room temperature to prevent adhesion to channel walls. Fresh blood samples were obtained from healthy donors (Mount Sinai Hospital, Toronto, Canada) and tested following the same procedure with the stored RBC samples. All samples were tested within one hour after incubation.

Experimental methods

The microfluidic device was constructed with PDMS using standard soft lithography, as described elsewhere.[32] The device consists of two layers of different thickness. The thickness of the testing areas is 8 μm, while the thickness of the loading channels is 50 μm for reducing flow resistance (ESI† Fig. S1). After the RBCs were loaded into the device inlet, a custom-developed water tank system applied pressure (2.5 kPa) to the cell loading channel and hydrodynamic focusing channels. The applied pressure of 2.5 kPa was chosen with considerations of testing throughput and the frame rate limitation of the high-speed camera. Cell images were captured at a speed of 5000 frames s^{-1} (416 pixel by 142 pixel) *via* a high-speed camera (HiSpec 1, Fastec Imaging Corp., U.S.), under a 60× objective of an inverted microscope (resolution: 0.23 μm $pixel^{-1}$). A standard halogen lamp was used to illuminate the region of interest under bright field imaging.

A custom-designed MATLAB image processing program was developed for automated RBC image analysis. For each video, the region of interest (ROI) is defined as the microchannel region excluding the PDMS area. After Gaussian filtering, canny edge detection with adaptive thresholding is applied to extract cell edges. All the edge points inside the ROI are accumulated along the X and Y axes, respectively. The peak regions in the X and Y curves indicate the coarse cell region, based on which the fine cell region is obtained by iterations of localizing the active contours of the cell. Length, width, area, and perimeter are measured for each RBC to quantify its DI, time constant (tc), and circularity.

Results and discussion

Hydrodynamic focusing efficiency

The shape of RBCs flowing through small capillaries is a function of flow rate, initial position relative to the central line of the capillary, and the diameter of the capillary.[26,33–35] For consistency, RBCs need to be centered in the microchannel and deformed symmetrically. If cells are asymmetrically deformed, the definition of DI = L/D becomes less appropriate for describing their deformation behavior[26] (see ESI† video S1 and S2). Experiments demonstrate that RBCs close to the central line of the microchannel reveal a more symmetrically deformed shape while cells near channel walls usually are asymmetrically deformed. Cells near the channel walls at the entrance typically stay near the channel wall until exiting the channel.

When RBCs enter the channel, their positions are random. Hence, hydrodynamic focusing near the inlet (see Fig. 1) was used to better position RBCs close to the central line of the microchannel for later RBC deformation measurement under shear stress. The usage of hydrodynamic focusing was also described elsewhere to center as well as apply forces to cells for deformation measurement.[36] Fig. 2 shows a histogram of central distance (*i.e.*, the distance between the cell center and the microchannel's central line) of RBCs before (blue) and after (red) the hydrodynamic focusing unit (n = 1500). The percentage of RBCs near the microchannel center was increased significantly by hydrodynamic focusing, and the number of cells more than two pixels away from the channel center was significantly reduced. The data presented in this paper only include those RBCs that were no more than two pixels away from the central line of the microchannel.

Time constant

After the RBC enters the recovery region, the time constant (tc) of each RBC is determined by fitting its DI values over

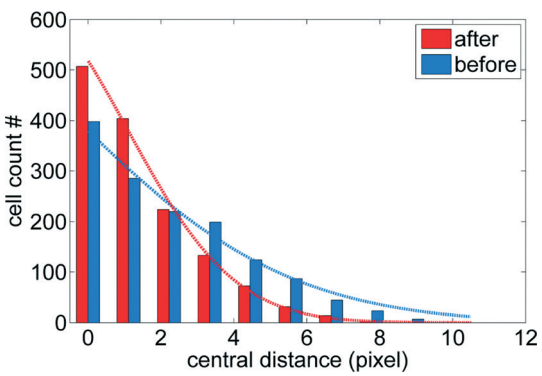

Fig. 2 Efficiency of hydrodynamic focusing. Histogram of central distance (*i.e.*, the distance between the center of the cell and microchannel's central line) of RBCs before (blue) and after (red) the focusing unit (n = 1500). Central distance of zero means the cell is perfectly centered within the microchannel. The percentage of RBCs near the microchannel center was increased significantly by hydrodynamic focusing.

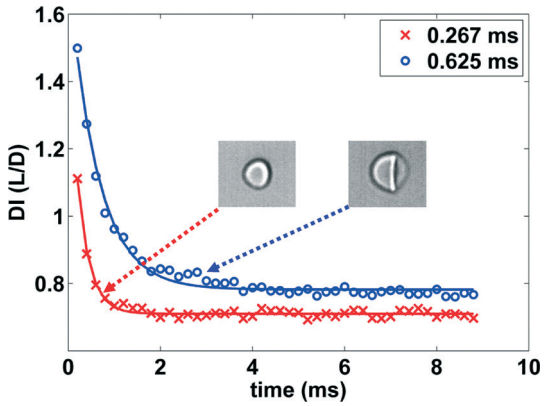

Fig. 3 Shape recovery of a biconcave RBC (blue) and spherical RBC (red) fitted to an exponential model. The spherical shape of the cell was due to morphological change during blood storage. Time constant (tc) of the spherical RBC (stored for 6 weeks) is 0.267 ms, and the tc value of the biconcave RBC (stored for 1 week) is 0.625 ms. The relationship between deformability change and morphology change is discussed in the next section.

time to an exponential function, in order to characterize the recovery rate of the cell. The exponential model is adapted from the standard Kelvin–Voigt model for describing the recovery properties of RBCs.[37,38] Fig. 3 shows two sets of data, one from a biconcave RBC (blue) and the other from a spherical RBC (red) due to storage (see ESI† video S1 and S3). The first data point on each curve was obtained from the image frame right after the cell exits the microchannel. For the RBCs shown in Fig. 3, time constant (tc) of the spherical RBC is 0.267 ms, while the tc value of the biconcave RBC is 0.625 ms.

It is worth noting that the time constant of RBCs reported in the literature was approximately 100 ms.[39–41] In contrast, the time constant we quantified ranges from 0.1 ms to 1 ms. In previous studies, DI was typically measured starting from 100 ms after an RBC was released from deformation until the shape completely recovered (several seconds).[39,40] In our experiments, enabled by high-speed imaging, the rapid recovery process was captured immediately after an RBC was released (within 10 ms, 50 frames in total at 5000 fps). During this period, RBCs recover much faster than in the later period (*e.g.*, after 100 ms as in earlier studies). As a result, the captured fast dynamics of RBC deformation more authentically revealed the cell shape recovery behavior, and exponential fitting resulted in time constant values orders of magnitude lower than those from earlier results in the literature.

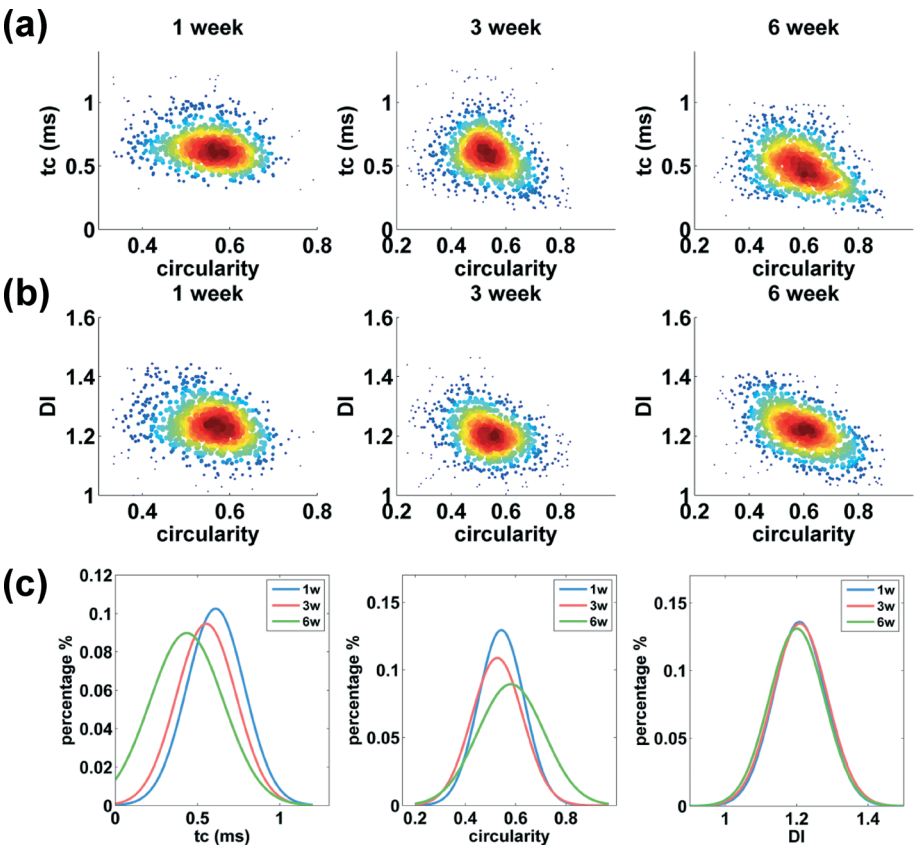

Fig. 4 (a)(b) Scatter plots of time constant *vs.* circularity; deformation index (DI) *vs.* circularity, for the same blood sample stored for 1 week (n = 1038), 3 weeks (n = 1027), and 6 weeks (n = 1001). (c) Distribution of time constant, circularity, and DI. Distribution curves were obtained by fitting the histogram of each RBC sample (see ESI† Fig. S2) to a normalized distribution function.

Changes in RBC deformation index, time constant, and circularity over blood storage

Fig. 4 summarizes results from testing the same blood sample stored for 1 week (n = 1038), 3 weeks (n = 1027), and 6 weeks (n = 1001). The scatter plots show tc *vs.* circularity [Fig. 4(a)] and DI *vs.* circularity [Fig. 4(b)]. Within each sample, both tc and DI show a decreasing trend as circularity increases, indicating that morphological changes of RBCs are a factor that causes RBC deformability changes over blood storage. Fig. 4(c) shows the distribution of these three parameters. It can be seen that the average time constant becomes lower as the RBCs are stored longer. The lower time constant may be attributed to ATP loss. It has been proven that the depletion of ATP alters its binding to spectrin–actin, which modifies RBC's cytoskeleton structure,[42–44] resulting in RBC stiffening and faster recovery.[39,45] During storage, RBCs undergo a number of biochemical changes, including ATP depletion,[46,47] which may be a cause of the lower time constants of older RBCs.

The average circularity of fresher and older RBCs is not significantly different; however, the distribution (*i.e.*, standard deviation) becomes wider. Thus, the distribution width of circularity (circularity-DW) can possibly be used as an indicator of stored RBC quality or age. The alteration of circularity distribution over time is mainly contributed by RBC morphology changes. Based on experimental observation, as stored RBCs age, they first swell and then progressively change to a sphere-like shape. A portion of the aged RBCs became more spherical, making their circularity approach one. There were also RBCs appearing isotropically enlarged from storage, and these RBCs typically revealed a higher DI value. When they pass through the microchannel, their deformed shape resulted in lower circularity. The more spherical cells and isotropically swelling cells increased circularity-DW.

No significant difference in DI was found (DI: 1.227 for 1 week, 1.221 for 3 week, and 1.219 for 6 week) [Fig. 4(c)]. This implies that when stored RBCs are transfused into patients, they are able to flow through microcapillaries with a similar *folding* capability. However, their stretching capability might become poorer, according to the lower elongation index (EI) measured with ektacytometry.[1,14–16] The insignificant folding DI change of older RBCs (*vs.* fresher RBCs) as quantified in our work, and the significant stretching EI change of older RBCs (*vs.* fresher RBCs) as reported in ektacytometry measurements can be due to the fundamentally different cell deformation modes.[29,30] Although the depletion of ATP alters RBC cytoskeleton, the stretching EI change might not be a concern in transfusion medicine since the stretching mode is not *in vivo* like and can be physiologically irrelevant.

We further investigated the effect of RBC morphology change (circularity) on time constant. Fig. 5 shows the

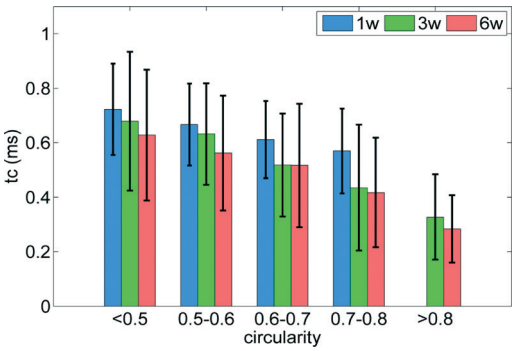

Fig. 5 Comparison of time constants for the same blood sample stored for 1 week (n = 1038), 3 weeks (n = 1027), and 6 weeks (n = 1001). Circularity is divided into five sub-ranges. Error bars represent standard deviation. In the last circularity range (>0.8), the group of 1 week old RBCs is not present because no RBC has a circularity higher than 0.8 in 1 week old sample.

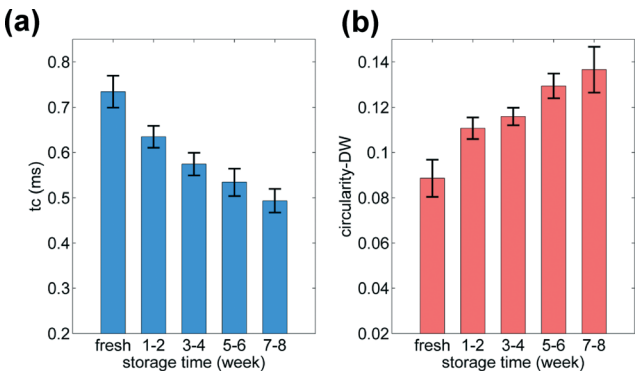

Fig. 6 Time constant (a) and circularity-DW (b) alteration over time. Each data point was obtained from 5 blood samples and over 1000 cells were tested within each sample. Significant differences exist between neighbor data points ($p < 0.05$). A relatively larger change between fresh and 1–2 week samples was found, compared to the steady changes over time during storage.

average and standard deviation of measured tc values within each circularity range (divided into five sub-ranges). Both fresher and older RBCs with higher circularity reveal lower time constant. Due to intrinsic property changes, within each circularity range, older RBCs show consistently lower time constants, compared to fresher RBCs.

Finally, five blood samples were tested from fresh to 8 weeks' storage, at time intervals of every two weeks ($n >$ 1000 per time interval per sample). As shown in Fig. 6 (individual data points are shown in ESI† Fig. S3), time constant decreases and circularity-DW (distribution width) increases over blood storage. Significant differences exist between neighboring data points ($p < 0.05$), demonstrating that time constant and circularity-DW can possible be used as indicators of RBC storage age or stored RBC quality. Standard deviations shown in Fig. 6 can be attributed to blood donor variations and variations in blood processing procedures.[48,49]

Conclusion

The deformability changes of stored red blood cells (RBCs) were studied using a human-capillary-like microfluidic channel. High-speed imaging system and automated image processing were used to quantify multiple parameters, enabling a higher measurement speed. Fresh and stored blood samples (up to 8 weeks) were tested. Besides large sample sizes, our study, for the first time, revealed deformation behavior changes of stored RBCs when traveling through human-capillary-like microchannels. Although existing literature consistently reported stretching deformability change of stored RBCs, our results show that no significant difference exists in their folding deformability. Furthermore, we report that significant changes in time constant (*i.e.*, recovery rate) and circularity distribution width (*i.e.*, heterogeneity of morphology) can be useful parameters for quantifying stored RBC quality or age.

Acknowledgements

Financial support from the Natural Sciences and Engineering Research Council of Canada (NSERC) through an E. W. R. Steacie Fellowship, from the University of Toronto through a Connaught Innovation Award, and from the Canada Research Chairs Program is acknowledged.

References

1 E. Bennett-Guerrero, T. H. Veldman, A. Doctor, M. J. Telen, T. L. Ortel, T. S. Reid, M. A. Mulherin, H. M. Zhu, R. D. Buck, R. M. Califf and T. J. McMahon, Evolution of adverse changes in stored RBCs *Proc. Natl. Acad. Sci. U. S. A.*, 2007, **104**, 17063–17068.

2 J. S. Lee and M. T. Gladwin, Bad Blood The risks of red cell storage *Nat. Med.*, 2010, **16**, 381–382.

3 C. Aubron, A. Nichol, D. J. Cooper and R. Bellomo, Age of red blood cells and transfusion in critically ill patients *Ann. Intensive Care*, 2013, **3**, 1–11.

4 M. J. Vandromme, G. McGwin and J. A. Weinberg, Blood transfusion in the critically ill: does storage age matter? *Scand. J. Trauma Resusc. Emerg. Med.*, 2009, **17**, 35.

5 T. L. Berezina, S. B. Zaets, C. Morgan, C. R. Spillert, M. Kamiyama, Z. Spolarics, E. A. Deitch and G. W. Machiedo, Influence of storage on red blood cell rheological properties *J. Surg. Res.*, 2002, **102**, 6–12.

6 A. B. Zimrin and J. R. Hess, Current issues relating to the transfusion of stored red blood cells *Vox Sang.*, 2009, **96**, 93–103.

7 C. G. Koch, L. Li, D. I. Sessler, P. Figueroa, G. A. Hoeltge, T. Mihaljevic and E. H. Blackstone, Duration of red-cell storage and complications after cardiac surgery *N. Engl. J. Med.*, 2008, **358**, 1229–1239.

8 J. Bonaventura, Clinical implications of the loss of vasoactive nitric oxide during red blood cell storage *Proc. Natl. Acad. Sci. U. S. A.*, 2007, **104**, 19165–19166.

9 J. D. Reynolds, G. S. Ahearn, M. Angelo, J. Zhang, F. Cobb and J. S. Stamler, S-nitrosohemoglobin deficiency: A mechanism for loss of physiological activity in banked blood *Proc. Natl. Acad. Sci. U. S. A.*, 2007, **104**, 17058–17062.

10 B. Blasi, A. D'Alessandro, N. Ramundo and L. Zolla, Red blood cell storage and cell morphology *Transfus. Med.*, 2012, **22**, 90–96.

11 P. L. La Celle, Alteration of deformability of the erythrocyte membrane in stored blood *Transfusion*, 1969, **9**, 238–245.

12 R. I. Weed, P. L. LaCelle and E. W. Merrill, Metabolic dependence of red cell deformability *J. Clin. Invest.*, 1969, **48**, 795–809.

13 R. R. Huruta, M. L. Barjas-Castro, S. T. O. Saad, F. F. Costa, A. Fontes, L. C. Barbosa and C. L. Cesar, Mechanical properties of stored red blood cells using optical tweezers *Blood*, 1998, **92**, 2975–2977.

14 S. M. Frank, B. Abazyan, M. Ono, C. W. Hogue, D. B. Cohen, D. E. Berkowitz, P. M. Ness and V. M. Barodka, Decreased Erythrocyte Deformability After Transfusion and the Effects of Erythrocyte Storage Duration *Anesth. Analg.*, 2013, **116**, 975–981.

15 S. Henkelman, M. J. Dijkstra-Tiekstra, J. de Wildt-Eggen, R. Graaff, G. Rakhorst and W. van Oeveren, Is red blood cell rheology preserved during routine blood bank storage? *Transfusion*, 2010, **50**, 941–948.

16 M. Uyuklu, M. Cengiz, P. Ulker, T. Hever, J. Tripette, P. Connes, N. Nemeth, H. J. Meiselman and O. K. Baskurt, Effects of storage duration and temperature of human blood on red cell deformability and aggregation *Clin. Hemorheol. Microcirc.*, 2009, **41**, 269–278.

17 E. Shojaei-Baghini, Y. Zheng, M. A. S. Jewett, W. B. Geddie and Y. Sun, Mechanical characterization of benign and malignant urothelial cells fromvoided urine *Appl. Phys. Lett.*, 2013, **102**, 123704.

18 M. Diez-Silva, M. Dao, J. Y. Han, C. T. Lim and S. Suresh, Shape and Biomechanical Characteristics of Human Red Blood Cells in Health and Disease *MRS Bull.*, 2010, **35**, 382–388.

19 D. H. Kim, P. K. Wong, J. Park, A. Levchenko and Y. Sun, Microengineered Platforms for Cell Mechanobiology *Annu. Rev. Biomed. Eng.*, 2009, **11**, 203–233.

20 R. T. Usry, G. L. Moore and F. W. Manalo, Morphology of stored, rejuvenated human erythrocytes *Vox Sang.*, 1975, **28**, 176–183.

21 M. Musielak, Red blood cell-deformability measurement: Review of techniques *Clin. Hemorheol. Microcirc.*, 2009, **42**, 47–64.

22 O. K. Baskurt, M. R. Hardeman, M. Uyuklu, P. Ulker, M. Cengiz, N. Nemeth, S. Shin, T. Alexy and H. J. Meiselman, Comparison of three commercially available ektacytometers with different shearing geometries *Biorheology*, 2009, **46**, 251–264.

23 M. Bessis and N. Mohandas, Laser Diffraction Patterns of Sickle Cells in Fluid Shear Fields *Blood Cells*, 1977, **3**, 229–239.

24 G. J. Streekstra, J. G. G. Dobbe and A. G. Hoekstra, Quantification of the fraction poorly deformable red blood

cells using ektacytometry *Opt. Express*, 2010, **18**, 14173–14182.
25 M. R. Clark, N. Mohandas and S. B. Shohet, Deformability of Oxygenated Irreversibly Sickled Cells *J. Clin. Invest.*, 1980, **65**, 189–196.
26 M. Abkarian, M. Faivre, R. Horton, K. Smistrup, C. A. Best-Popescu and H. A. Stone, Cellular-scale hydrodynamics *Biomed. Mater.*, 2008, **3**, 034011.
27 J. H. Jeong, Y. Sugii, M. Minamiyama and K. Okamoto, Measurement of RBC deformation and velocity in capillaries in vivo *Microvasc. Res.*, 2006, **71**, 212–217.
28 T. Ye, H. Li and K. Y. Lam, Modeling and simulation of microfluid effects on deformation behavior of a red blood cell in a capillary *Microvasc. Res.*, 2010, **80**, 453–463.
29 R. M. Hochmuth and R. E. Waugh, Erythrocyte-Membrane Elasticity and Viscosity *Annu. Rev. Physiol.*, 1987, **49**, 209–219.
30 E. Evans, N. Mohandas and A. Leung, Static and Dynamic Rigidities of Normal and Sickle Erythrocytes - Major Influence of Cell Hemoglobin Concentration *J. Clin. Invest.*, 1984, **73**, 477–488.
31 M. E. Brecher, *AABB Technical Manual*, AABB Press, Bethesda, 2005.
32 Y. Zheng, E. Shojaei-Baghini, C. Wang and Y. Sun, Microfluidic characterization of specific membrane capacitance and cytoplasm conductivity of single cells *Biosens. Bioelectron.*, 2013, **42**, 496–502.
33 T. W. Secomb, B. Styp-Rekowska and A. R. Pries, Two-dimensional simulation of red blood cell deformation and lateral migration in microvessels *Ann. Biomed. Eng.*, 2007, **35**, 755–765.
34 G. Tomaiuolo, M. Simeone, V. Martinelli, B. Rotoli and S. Guido, Red blood cell deformation in microconfined flow *Soft Matter*, 2009, **5**, 3736–3740.
35 Y. Zheng, J. Nguyen, C. Wang and Y. Sun, Electrical measurement of red blood cell deformability on a microfluidic device *Lab Chip*, 2013, **13**, 3275–3283.
36 J. S. Dudani, D. R. Gossett, H. T. K. Tse and D. Di Carlo, Pinched-flow hydrodynamic stretching of single-cells *Lab Chip*, 2013, **13**, 3728–3734.
37 E. A. Evans, New Membrane Concept Applied to Analysis of Fluid Shear-Deformed and Micropipet-Deformed Red Blood-Cells *Biophys. J.*, 1973, **13**, 941–954.
38 R. M. Hochmuth, P. R. Worthy and E. A. Evans, Red-Cell Extensional Recovery and the Determination of Membrane Viscosity *Biophys. J.*, 1979, **26**, 101–114.
39 S. Braunmuller, L. Schmid, E. Sackmann and T. Franke, Hydrodynamic deformation reveals two coupled modes/time scales of red blood cell relaxation *Soft Matter*, 2012, **8**, 11240–11248.
40 K. B. Roth, C. D. Eggleton, K. B. Neeves and D. W. M. Marr, Measuring cell mechanics by optical alignment compression cytometry *Lab Chip*, 2013, **13**, 1571–1577.
41 G. Tomaiuolo, M. Barra, V. Preziosi, A. Cassinese, B. Rotoli and S. Guido, Microfluidics analysis of red blood cell membrane viscoelasticity *Lab Chip*, 2011, **11**, 449–454.
42 S. Manno, Y. Takakuwa and N. Mohandas, Modulation of erythrocyte membrane mechanical function by protein 4.1 phosphorylation *J. Biol. Chem.*, 2005, **280**, 7581–7587.
43 T. Betz, M. Lenz, J. F. Joanny and C. Sykes, ATP-dependent mechanics of red blood cells *Proc. Natl. Acad. Sci. U. S. A.*, 2009, **106**, 15320–15325.
44 H. Y. Chu, E. Puchulu-Campanella, J. A. Galan, W. A. Tao, P. S. Low and J. F. Hoffman, Identification of cytoskeletal elements enclosing the ATP pools that fuel human red blood cell membrane cation pumps *Proc. Natl. Acad. Sci. U. S. A.*, 2012, **109**, 12794–12799.
45 N. S. Gov and S. A. Safran, Red blood cell membrane fluctuations and shape controlled by ATP-induced cytoskeletal defects *Biophys. J.*, 2005, **88**, 1859–1874.
46 H. K. Jindal, Z. W. Ai, P. Gascard, C. Horton and C. M. Cohen, Specific loss of protein kinase activities in senescent erythrocytes *Blood*, 1996, **88**, 1479–1487.
47 M. Girasole, G. Pompeo, A. Cricenti, G. Longo, G. Boumis, A. Bellelli and S. Amiconi, The how, when, and why of the aging signals appearing on the human erythrocyte membrane: an atomic force microscopy study of surface roughness *Nanomed.: Nanotechnol., Biol. Med.*, 2010, **6**, 760–768.
48 D. Devine, Processing of Whole Blood into Cellular Components and Plasma *Vox Sang.*, 2010, **99**, 26–26.
49 Y. Yu, C. Ma, Q. Feng, L. Chen, H. Li, Y. Zhuang and D. Wang, Optimization of Preparation Technology of Internal Quality Control Products for Blood Transfusion Compatibility Testing *Vox Sang.*, 2012, **103**, 81–82.